Characterization of the Basal Ganglia Using Diffusion Tensor Imaging in Children with Self-Injurious Behavior and Tuberous Sclerosis Complex

Tanjala T. Gipson, Andrea Poretti, Sarah A. Kelley, Kathryn A. Carson, Michael V. Johnston, Thierry A.G.M. Huisman

From the Department of Pediatrics, University of Tennessee Health Sciences Center, Memphis, TN (TTG); Le Bonheur Children's Hospital and Boling Center for Developmental Disabilities, Memphis, TN (TTG); Division of Pediatric Radiology and Pediatric Neuroradiology, Department of Radiology and Radiological Sciences, Johns Hopkins University School of Medicine, Baltimore, MD (AP, TAGMH); Departments of Neurology and Pediatrics, Johns Hopkins University School of Medicine, Baltimore, MD (SAK); Department of Epidemiology, Johns Hopkins Bloomberg School of Public Health, Baltimore, MD (KAC); Johns Hopkins University School of Medicine, Baltimore, MD (KAC); and Departments of Pediatrics, Neurology, Physical Medicine, and Rehabilitation, Johns Hopkins University School of Medicine, Baltimore, MD (MVJ).

ABSTRACT

BACKGROUND AND PURPOSE: **Tuberous sclerosis complex (TSC) is a rare, genetic disease that is associated with multiple manifestations including epilepsy and autism. Self-injurious behaviors (SIBs) also occur in a subset of patients. This study used diffusion tensor imaging (DTI) in children with TSC for quantitative and volumetric analysis of brain regions that have been associated with SIB in other genetic conditions.**

METHODS: **We used DTI to compare 6 children with TSC-associated SIB and 10 children with TSC without SIB. Atlas-based analysis of DTI data and calculation of number of voxels; fractional anisotropy (FA); and mean, axial, and radial diffusivity were performed for multiple regions; DTI measures were summarized using medians and interquartile ranges and were compared using Wilcoxon rank sum tests and false discovery rates (FDRs).**

RESULTS: **Analysis showed that children with TSC and SIB had reduced numbers of voxels (median) in the bilateral globus pallidus (right: 218 vs. 260, $P = .008$, FDR = .18; left: 222 vs. 274, $P = .002$, FDR = .12) and caudate nucleus (right: 712 vs. 896, $P = .01$, FDR = .26; left: 702 vs. 921, $P = .03$, FDR = .44) and reduced FA in the bilateral globus pallidus (right: .233 vs. .272, $P = .003$, FDR = .12; left: .223 vs. .247, $P = .004$, FDR = .12) and left caudate nucleus (.162 vs. .186, $P = .03$, FDR = .39) versus children without SIB. No other statistically significant differences were found.**

CONCLUSIONS: **These data support a correlation between lower volumes of the globus pallidus and caudate with SIB in children with TSC.**

Keywords: Tuberous sclerosis complex, diffusion tensor imaging, behavior, self-injurious behavior, autism, intellectual disability.

Acceptance: Received August 22, 2018. Accepted for publication April 24, 2019.

Correspondence: Address correspondence to Tanjala T. Gipson, MD, Boling Center for Developmental Disabilities, 711 Jefferson Avenue, Memphis, TN 38103. E-mail: tgipson@uthsc.edu.

Author A. Poretti is deceased.

Acknowledgments and Disclosure: The authors thank Jeffrey Baum for his assistance with data collection. Writing assistance was provided by Robert Schoen, PharmD, and Traci Stuve, MA (ApotheCom, Yardley, PA, USA), and supported by Novartis. K. A. Carson's work on the project was funded by the Johns Hopkins Institute for Clinical and Translational Research, under grant number UL1 TR001079 from the National Center for Advancing Translational Sciences, a component of the National Institutes of Health (NIH) and the NIH Roadmap for Medical Research. T. T. Gipson's work on the project was supported by grant number 2K12NS001696-11A from the National Institute of Neurological Disorders and Stroke. A. Poretti, S. A. Kelley, M. V. Johnston, and T. A. G. M. Huisman report no conflicts of interest. Funding for editorial support was provided by Novartis Pharmaceuticals.

J Neuroimaging 2019;29:506-511.
DOI: 10.1111/jon.12628

Introduction

Tuberous sclerosis complex (TSC) is a rare disease that may be inherited (autosomal dominant) or develop spontaneously with an overall incidence of 1 per 6,000 live births.[1–3] Epilepsy is present in as many as 90%,[4,5] autism in up to 60%,[6,7] and self-injurious behavior (SIB) in 10-41% of children.[8] SIBs are chronic and repetitious self-directed behavioral actions that result in physical harm and may lead to tissue damage or tissue loss.[9] When SIB is detected in individuals with TSC, it may represent a particularly severe phenotype of autism and/or intellectual disability.[10] The prevalence of SIB in TSC was reported similar to SIB in other genetic conditions in a questionnaire-based study.[8] The pathophysiology of SIB in TSC remains unknown; however, Pryor et al discovered that striatal deletion of the TSC1 gene was associated with premature death and rapid development of motor impairments, and that overexpression of the huntingtin protein in the striatum was associated with increased mammalian target of rapamycin (mTOR) activity,[11] which is also implicated in TSC.[12,13]

SIB has been localized or linked to abnormalities of the basal ganglia in patients with Lesch-Nyhan syndrome,[14,15] and in preclinical models.[16] The basal ganglia have been characterized across several study types in TSC. Isik et al described the growth of subependymal giant cell astrocytomas in the basal

ganglia of two infants with TSC.[17] Whole-brain mapping in individuals with TSC revealed a predominance of subependymal nodules in association with the caudate nucleus.[18] Functionally, working memory impairments in TSC were associated with basal ganglia lesions, along with other cortical regions.[19] Hemichorea was associated with unilateral basal ganglia atrophy in an individual with TSC.[20] Generalized chorea in TSC was reported with and without bilateral basal ganglia involvement.[21–23] Interestingly, abnormalities in glutamate and gamma-aminobutyric acid, both of which are major neurotransmitters in the functionality of the basal ganglia, are well described in TSC.[24,25]

The goal of our study was to investigate the role of the basal ganglia in SIB associated with TSC by employing diffusion tensor imaging (DTI). DTI allows for noninvasive study of the anatomic and functional neuroarchitecture and renders both qualitative and quantitative scalars as well as volumetric analysis. DTI has been applied in the exploration of multiple neurologic diseases in children; for example, DTI has been used to characterize language in the TSC population.[26]

Clinically, we observed that SIB rarely resolves with traditional intervention. In one study, SIB persisted in 84.6% of patients.[27] In our center, we gathered behavioral and medical data for over a year on a patient with TSC-associated SIB and aggression noting a decrease in SIB primarily with the mTOR inhibitor everolimus.[28] Therefore, we surmised that SIB in TSC may be related to localized dysregulation of the protein kinase mTOR. We hypothesize that SIB in TSC may represent a localizable subphenotype of autism in TSC. To test this hypothesis and generate preliminary data for a larger study, we investigated children with TSC and SIB for volumetric and microstructural changes of the basal ganglia as compared with children who have TSC without SIB.

Methods

This retrospective study was approved by the Johns Hopkins Medicine Institutional Review Board. Because of the retrospective nature of this study and its absence of risk, a consent waiver was granted.

Participants

The inclusion criteria for this study were confirmed diagnosis of TSC based on the 2012 revised diagnostic criteria,[1] availability of DTI data without artifacts enabling a high-quality DTI postprocessing, and age at the time of magnetic resonance imaging (MRI) 2–18 years. Demographic data, detailed information about the TSC phenotype and genotype, and diagnoses of SIB were collected by review of the clinical charts and/or comprehensive history and physical examination by one of the investigators (SK or TG). Cognitive development was assessed based on the child's ability to complete activities of daily living for their chronologic age. Patients were diagnosed with SIB if they engaged in persistent, damaging skin picking or pulling, self-biting, or self-hitting beyond head banging only. Children with head banging only were not included in the study because this could be considered typical pediatric behavior, although no patients had to be excluded for this reason in our cohort. Data are from eligible patients who were seen at the Tuberous Sclerosis Clinic at the Kennedy Krieger Institute, Baltimore, MD, or at the Division of Pediatric Neurology at Johns Hopkins Children's Center, Baltimore, MD, between October 1, 2010, and May 31, 2014.

MRI Acquisition

All MRI studies were performed on a 1.5T Avanto scanner (Siemens Medical Solutions, Erlangen, Germany) using standard departmental protocol for patients with TSC, including 3-dimensional (3D) T1-weighted and axial T2-weighted images; an axial fluid-attenuated inversion recovery sequence; axial, coronal, and sagittal T1-weighted images after intravenous injection of gadolinium-based contrast agent; and a single-shot, spin-echo, echo-planar axial DTI sequence with diffusion gradients along 20 noncollinear directions. For the 3D T1-weighted images, we used the following acquisition parameters: repetition time of 1,130 milliseconds, echo time of 3.99 milliseconds, slice thickness of 1.0 mm, with an in-plane pixel size of .99 mm × .99 mm. For the acquisition of DTI data, we used an effective, high b value of 1,000 second/mm^2 for each of the 20 diffusion-encoding directions. We performed an additional measurement without diffusion weighting ($b = 0$ second/mm^2). For the acquisition of the DTI data, the following parameters were used: repetition time of 7,100 milliseconds, echo time of 84 milliseconds, slice thickness of 2.5 mm, field of view of 240 × 240 mm, and matrix size of 192 × 192. Parallel imaging was performed using integrated parallel acquisition technique (iPAT) = 2 with generalized, autocalibrating, partially parallel acquisition reconstruction. The acquisition was repeated twice to enhance the signal-to-noise ratio.

DTI Analysis

All DTI data sets were processed offline by using DtiStudio, DiffeoMap, and RoiEditor software (H. Jiang and S. Mori, Johns Hopkins University (JHU), Baltimore, MD; freely available at www.MriStudio.org). After correcting for eddy currents and motion artifacts, all images were coregistered to each other by using a 12-mode affine-automated image registration transformation. Subsequently, the following DTI maps and images were generated: fractional anisotropy (FA), color-coded FA, trace of diffusion, axial diffusivity (AD), and radial diffusivity (RD). After skull-stripping, the images were subsequently normalized to the Montreal Neurological Institute (MNI) coordinates by using a nine-parameter affine linear automated image registration transformation. For this transformation, $b0$ images were used for both the subject data and the JHU-MNI "Eve" template. Subsequently, a nonlinear transformation was applied by using dual-contrast (FA and trace of diffusion) large deformation diffeomorphic metric mapping. Finally, atlas-based analysis was performed by using a white matter parcellation map of the JHU-MNI Eve template,[29,30] and the brain was parcellated into 189 anatomic regions, including both gray and white matter. Because of the reciprocal nature of both linear and nonlinear transformation, the transformation results were used to warp the white matter parcellation map to the original DTI data, thus automatically segmenting each brain into the 189 subregions. FA, mean diffusivity (MD; calculated as trace of diffusion divided by 3), AD, and RD were calculated for the following bilateral brain regions: amygdala, caudate nucleus, putamen, globus pallidus, nucleus accumbens, hippocampus, hypothalamus, postcentral gyrus, and superior parietal gyrus. These regions were selected because they have been associated with SIB in the literature.[16,31–34]

Table 1. Demographic and Clinical Characteristics of Patients with TSC with and without Self-Injurious Behavior

Characteristic	TSC with SIB $n = 6$	TSC without SIB $n = 10$	*P* Value
Sex, *n* (%)			.31
Male	5 (83)	5 (50)	
Female	1 (17)	5 (50)	
Mean (SD) age at MRI, years	9.0 (4.0)	8.8 (5.0)	.94
Range (min, max), years	4.1, 14.5	2.1, 17.5	
Cognitive development, *n* (%)			.03
Delayed	6 (100)	4 (40)	
Typical	0 (0)	6 (60)	
Genetic mutation, *n* (%)			.18
TSC1/truncating	0 (0)	1 (10)	
TSC1/frameshift	1 (17)	0 (0)	
TSC2/truncating	1 (17)	0 (0)	
TSC2/frameshift	0 (0)	1 (10)	
TSC2/missense	1 (17)	0 (0)	
TSC2/unknown	1 (17)	1 (100)	
NT	2 (33)	7 (70)	

MRI = magnetic resonance imaging; NT = not tested; SD = standard deviation; SIB = self-injurious behavior; TSC = tuberous sclerosis complex.

Volumetric Analysis

Volumetric analysis was performed by using the 3D T1-weighted data set, and postprocessing was executed similarly to the DTI analysis. For nonlinear transformation, a single-contrast large deformation diffeomorphic metric mapping was applied. The brain was parcellated into 189 anatomic regions, and the number of voxels was calculated for each brain subregion. For further analysis, we used the number of voxels of the same brain regions that were used for DTI (amygdala, caudate nucleus, putamen, globus pallidus, nucleus accumbens, hippocampus, hypothalamus, postcentral gyrus, and superior parietal gyrus). The voxel-based approach was based on a protocol as described by Dr. Mori et al.[35]

Statistical Methods

Demographic and clinical characteristics of patients with TSC with and without SIB were summarized using counts and percentages or mean and standard deviation and compared using Fisher exact test or a 2-sample *t* test, as appropriate. Nonparametric statistics were used to summarize and compare the DTI measures across groups. Specifically, DTI measures were summarized using medians and interquartile ranges (IQRs) and the two groups were compared using Wilcoxon rank sum tests. The analysis was exploratory; therefore, no correction was made for multiple comparisons. False discovery rates (FDRs) are reported for comparisons of DTI measures. Analysis was performed using SAS version 9.4 (SAS Institute Inc., Cary, NC, USA). All reported *P* values are 2-sided, and significance was set at $P < .05$.

Results

We included six children with TSC and SIB (five boys, mean age 9.0 ± 4.0 years) and 10 children with TSC without SIB (five boys, mean age 8.8 ± 5.0 years) who met our eligibility criteria. Demographic and clinical characteristics for the two groups are presented in Table 1. Of the patients who had TSC genotyping, 1 in each group had a TSC1 mutation, whereas 3 patients in the SIB group and 2 in the without SIB group had a TSC2 mutation. Age at MRI was similar between the groups. The children with

Table 2. Diffusion Tensor Imaging and MRI Measures for Patients with Tuberous Sclerosis Complex by Self-Injurious Behavior Status

Region	TSC with SIB $n = 6$	TSC without SIB $n = 10$	*P* Value	FDR
Globus pallidus right:				
Number of voxels	218 (203-222)	260 (252-316)	.008	.18
FA	.233 (.226-.246)	.272 (.265-.277)	.003	.12
MD ($\times 10^{-3}$ mm/second^2)	.839 (.830-.842)	.828 (.818-.870)	.79	1.0
AD ($\times 10^{-3}$ mm/second^2)	1.060 (1.051-1.084)	1.077 (1.049-1.085)	.55	1.0
RD ($\times 10^{-3}$ mm/second^2)	.722 (.718-.727)	.706 (.698-.765)	.70	1.0
Globus pallidus left:				
Number of voxels	222 (215-233)	274 (248-288)	.002	.12
FA	.223 (.203-.231)	.247 (.238-.264)	.004	.12
MD ($\times 10^{-3}$ mm/second^2)	.820 (.796-.831)	.822 (.813-.832)	.99	1.0
AD ($\times 10^{-3}$ mm/second^2)	1.007 (.996-1.022)	1.032 (1.004-1.040)	.14	1.0
RD ($\times 10^{-3}$ mm/second^2)	.723 (.701-.741)	.719 (.699-.731)	.55	1.0
Caudate nucleus right:				
Number of voxels	712 (619-814)	896 (831-981)	.01	.26
FA	.163 (.150-.192)	.184 (.161-.198)	.21	1.0
MD ($\times 10^{-3}$ mm/second^2)	.870 (.856-.892)	.849 (.810-.885)	.25	1.0
AD ($\times 10^{-3}$ mm/second^2)	1.026 (1.017-1.030)	1.001 (.951-1.032)	.30	1.0
RD ($\times 10^{-3}$ mm/second^2)	.800 (.772-.825)	.773 (.726-.800)	.18	1.0
Caudate nucleus left:				
Number of voxels	702 (655-841)	921 (836-964)	.03	.44
FA	.162 (.154-.170)	.186 (.174-.198)	.03	.39
MD ($\times 10^{-3}$ mm/second^2)	.840 (.828-.878)	.844 (.799-.853)	.48	1.0
AD ($\times 10^{-3}$ mm/second^2)	.993 (.979-1.028)	.978 (.954-1.006)	.36	1.0
RD ($\times 10^{-3}$ mm/second^2)	.765 (.750-.803)	.769 (.722-.776)	.48	1.0

AD = axial diffusivity; FA = fractional anisotropy; FDR = false discovery rate; MD = mean diffusivity; MRI = magnetic resonance imaging; RD = radial diffusivity; SIB = self-injurious behavior; TSC = tuberous sclerosis complex.
Results presented are median and interquartile range, and the *P* value is from the Wilcoxon rank sum test.

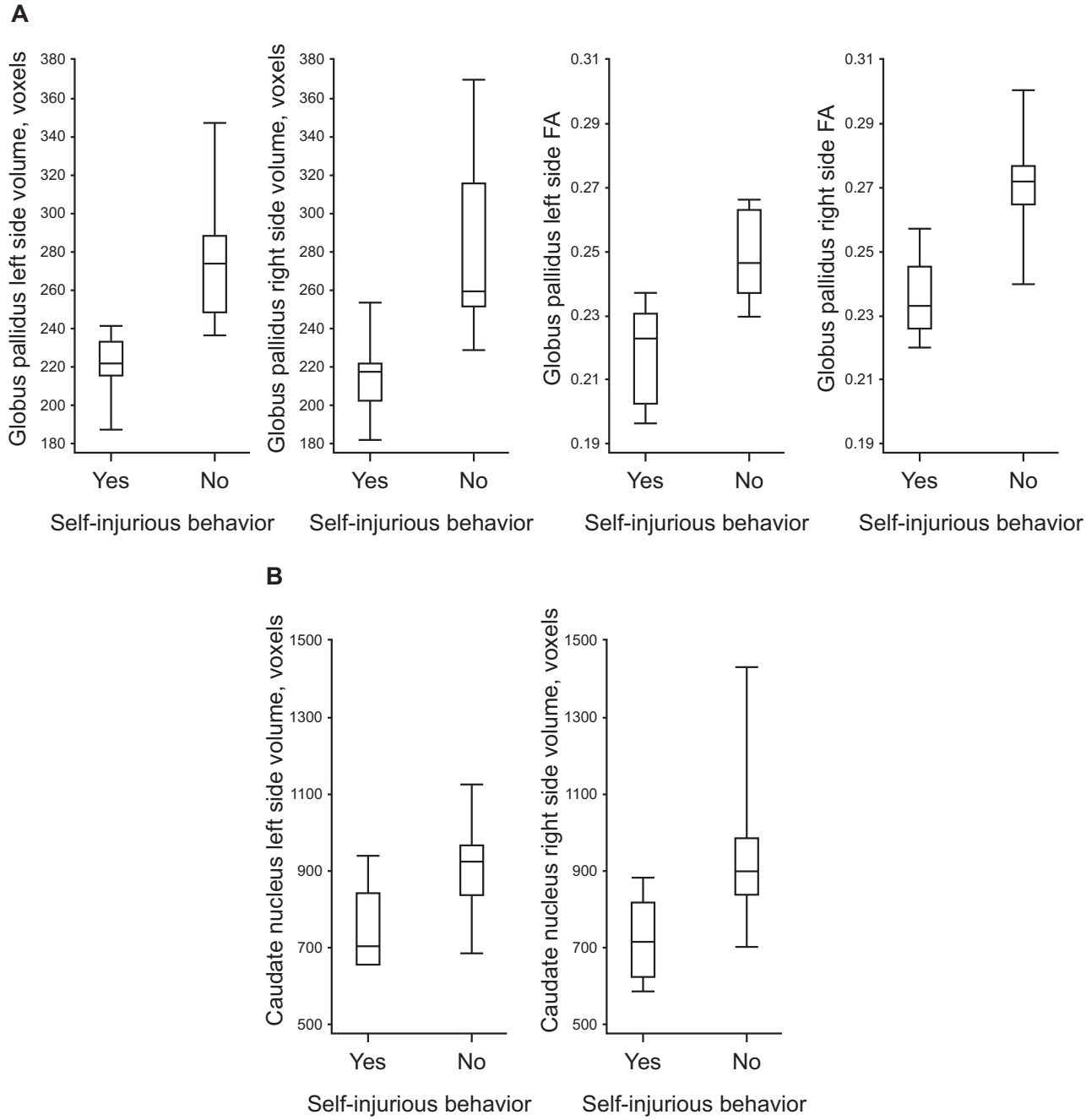

Fig 1. Box plots of DTI scalars that were significantly different by self-injurious behavior for the (A) globus pallidus and (B) caudate nucleus. Note: The middle line in the box represents the median value, the ends of the box represent the 25th and 75th percentiles, and the whiskers represent the 5th and 95th percentiles.

SIB were significantly more likely to have delayed cognitive development compared with the children without SIB.

Median and IQR of the number of voxels and FA in the globus pallidus and caudate nucleus regions are presented in Table 2. In children with TSC and SIB, we found a statistically significantly reduced number of voxels for the bilateral globus pallidus and caudate nucleus compared with children with TSC without SIB. Similarly, we found reduced FA for the bilateral globus pallidus and left caudate nucleus in children with TSC and SIB compared with children with TSC without SIB (Fig 1). The observed FA difference ranging from 10.8% to 16.7% is large enough for clinical use when measured quantitatively. The FA in the right caudate nucleus did not significantly differ between the groups, nor were there any statistically significant differences between the groups in the MD, AD, or RD measures for the globus pallidus or caudate nucleus regions (Table 2). Importantly, measured or evaluated anatomic regions had no focal findings noted or visible on conventional T1, T2, and fluid-attenuated inversion recovery MR imaging. We performed the same analysis on the putamen, amygdala, nucleus accumbens, hippocampus, hypothalamus, postcentral gyrus, and superior parietal gyrus regions and found no statistically significant differences in number of voxels, FA, MD, AD, or RD between the groups (data not shown).

Discussion

TSC is a lifelong chronic disease that requires vigilant monitoring for the development of systemic tumors, often necessitates interventions or multiple medications to alleviate intractable seizures, and carries a risk of inheritance. The development of SIB can be devastating for affected individuals and their families, and there is no cure. Localizing anatomic regions linked to SIB as a starting point for generating further studies and possible interventions that provide hope for improving the outcome is the final goal of this line of research.

Results from this DTI study characterize the basal ganglia (globus pallidus and caudate nucleus) as a potential component in SIB associated with TSC. The preliminary data generated by this study expand on our clinical experience by including low-functioning individuals with TSC and suggest that DTI may serve as a useful objective biomarker for the many individuals with TSC in whom it is difficult to obtain traditional outcome measures.[28]

While there is a lack of information on this topic in the TSC literature, the notion of SIB associated with basal ganglia anomaly or dysfunction is not novel. Lesch-Nyhan syndrome, the prototypical condition associated with SIB, has been linked to dopamine deficits in the basal ganglia without apparent neuropathologic abnormalities.[14,15] Pemoline-induced SIB has been associated with abnormally low neuronal metabolic activity of the caudate, putamen, and portions of the hypothalamus, and increased intensity of tissue injury followed exposure to stress.[16] In a 10-year-old boy with Lesch-Nyhan syndrome, pallidal deep-brain stimulation resulted in complete remission of SIB.[36] It is hoped that SIB in TSC may be likewise treatable despite its historic characterization as a static, irreversible condition. More research is required to establish a mechanism in TSC.

In the current study, DTI indicated a reduced volume and reduced FA in the bilateral globus pallidus and left caudate nucleus in children with TSC and SIB compared with children with TSC without SIB. Changes in FA values in gray matter are still poorly understood. FA metrics are best characterized in white matter, where FA values allow quantification of the directionality of diffusion on a microstructural level.[37] Within the gray matter, the principally cellular microstructure typically has predominant isotropic diffusion characteristics that are best evaluated by apparent diffusion coefficient (ADC) maps.[38] However, multiple studies have shown that FA values, markers of anisotropic diffusion, may also alter the microstructural anatomy if affected by a diffuse process.[39–42] For example, in patients with a cortical stroke, the FA values may increase within the cortical gray matter, likely secondary to a combination of cytotoxic and vasogenic edema impacting the diffusion of water molecules within the extracellular space.[39] Further analysis in future studies analyzing this component of altered diffusion appears indicated.

Limitations of our current study include the small sample size. We did observe differences that were statistically significant; however, the FDR for these significant differences ranged from 12% to 44%. Lack of statistically significant association with the hippocampi or the other evaluated structures may be secondary to the small sample size or may reflect anatomic structures that are not related to SIB. In this initial study, we did not ascertain whether total gray or white matter volume differences could also be correlated with SIB. Prior and concurrent medication use that may potentially affect brain volume or the size of nearby TSC lesions (such as mTOR inhibitors) was not accounted for. However, there were no subependymal giant cell astrocytomas localized to the basal ganglia that would have an impact on our analysis. Analyses also did not account for varying levels of cognitive disability or intracranial content volume. Although there were more patients with TSC2 mutations in the group with SIB than without, the small number of patients with known TSC mutations in the study limits the generalizability of the results. To our knowledge, no specific mutations/deletions in the TSC gene have been associated with SIB to date. It should be noted that iron deposition within central gray matter may impact the reliability of the collected DTI metrics secondary to the susceptibility artifacts/local magnetic field distortion. However, all DTI images were visually inspected for image distortion or focal signal loss and no pattern was seen. Future studies could include further MRI analysis to explain our isolated finding of significantly reduced FA as compared with MD, RD, and AD. Although differences in laterality in gray matter diffusivity in healthy individuals have been noted previously, including the caudate nucleus,[43] the significance of the unilaterality of our findings in the caudate nucleus is unknown. This may be an area for future research. Future studies should also include genetic analyses and examine correlations of the neurodevelopmental phenotype and clinical treatment outcomes in a larger treatment population of individuals followed over time.

References

1. Northrup H, Krueger DA. Tuberous sclerosis complex diagnostic criteria update: recommendations of the 2012 International Tuberous Sclerosis Complex Consensus Conference. Pediatr Neurol 2013;49:243-54.
2. Franz DN, Bissler JJ, McCormack FX. Tuberous sclerosis complex: neurological, renal and pulmonary manifestations. Neuropediatrics 2010;41:199-208.
3. Dixon BP, Hulbert JC, Bissler JJ. Tuberous sclerosis complex renal disease. Nephron Exp Nephrol 2011;118:e15-20.
4. Saxena A, Sampson JR. Epilepsy in tuberous sclerosis: phenotypes, mechanisms, and treatments. Semin Neurol 2015;35:269-76.
5. Chu-Shore CJ, Major P, Camposano S, et al. The natural history of epilepsy in tuberous sclerosis complex. Epilepsia 2010;51:1236-41.
6. Webb DW, Fryer AE, Osborne JP. Morbidity associated with tuberous sclerosis: a population study. Dev Med Child Neurol 1996;38:146-55.
7. Gillberg IC, Gillberg C, Ahlsen G. Autistic behaviour and attention deficits in tuberous sclerosis: a population-based study. Dev Med Child Neurol 1994;36:50-6.
8. Eden KE, de Vries PJ, Moss J, et al. Self-injury and aggression in tuberous sclerosis complex: cross syndrome comparison and associated risk markers. J Neurodev Disord 2014;6:10.
9. Hyman SL, Fisher W, Mercugliano M, et al. Children with self-injurious behavior. Pediatrics 1990;85:437-41.
10. Gipson TT, Gerner G, Wilson MA, et al. Potential for treatment of severe autism in tuberous sclerosis complex. World J Clin Pediatr 2013;2:16-25.
11. Pryor WM, Biagioli M, Shahani N, et al. Huntingtin promotes mTORC1 signaling in the pathogenesis of Huntington's disease. Sci Signal 2014;7:ra103.
12. Budde K, Gaedeke J. Tuberous sclerosis complex-associated angiomyolipomas: focus on mTOR inhibition. Am J Kidney Dis 2012;59:276-83.
13. Crino PB, Nathanson KL, Henske EP. The tuberous sclerosis complex. N Engl J Med 2006;355:1345-56.

14. Schroeder SR, Oster-Granite ML, Berkson G, et al. Self-injurious behavior: gene-brain-behavior relationships. Ment Retard Dev Disabil Res Rev 2001;7:3-12.
15. Visser JE, Bar PR, Jinnah HA. Lesch-Nyhan disease and the basal ganglia. Brain Res Brain Res Rev 2000;32:449-75.
16. Muehlmann AM, Kies SD, Turner CA, et al. Self-injurious behaviour: limbic dysregulation and stress effects in an animal model. J Intellect Disabil Res 2012;56:490-500.
17. Isik U, Dincer A, Sav A, et al. Basal ganglia location of subependymal giant cell astrocytomas in two infants. Pediatr Neurol 2010;42:157-9.
18. Katz JS, Milla SS, Wiggins GC, et al. Intraventricular lesions in tuberous sclerosis complex: a possible association with the caudate nucleus. J Neurosurg Pediatr 2012;9:406-13.
19. Ridler K, Suckling J, Higgins NJ, et al. Neuroanatomical correlates of memory deficits in tuberous sclerosis complex. Cerebral Cortex 2007;17:261-71.
20. Ferlazzo E, Gasparini S, Gambardella A, et al. Unilateral basal ganglia atrophy in a patient with tuberous sclerosis complex and hemichorea. Mov Disord 2012;27:458-60.
21. Evans BK, Jankovic J. Tuberous sclerosis and chorea. Ann Neurol 1983;13:106-7.
22. Wright RA, Pollock M, Donaldson IM. Chorea and tuberous sclerosis. Mov Disord 1992;7:87-9.
23. Chakravarty A, Basu S. An unusual case of tuberous sclerosis with family study. J Assoc Physicians India 1988;36:173-5.
24. Talos DM, Sun H, Kosaras B, et al. Altered inhibition in tuberous sclerosis and type IIb cortical dysplasia. Ann Neurol 2012;71:539-51.
25. Zeng LH, Ouyang Y, Gazit V, et al. Abnormal glutamate homeostasis and impaired synaptic plasticity and learning in a mouse model of tuberous sclerosis complex. Neurobiol Dis 2007;28:184-96.
26. Lewis WW, Sahin M, Scherrer B, et al. Impaired language pathways in tuberous sclerosis complex patients with autism spectrum disorders. Cereb Cortex 2013;23:1526-32.
27. Wilde L, Wade K, Eden K, et al. Persistence of self-injury, aggression and property destruction in children and adults with tuberous sclerosis complex. J Intellect Disabil Res 2018;62:1058-71.
28. Gipson TT, Jennett H, Wachtel L, et al. Everolimus and intensive behavioral therapy in an adolescent with tuberous sclerosis complex and severe behavior. Epilepsy Behav Case Rep 2013;1:122-5.
29. Jiang H, van Zijl PC, Kim J, et al. DtiStudio: resource program for diffusion tensor computation and fiber bundle tracking. Comput Methods Programs Biomed 2006;81:106-16.
30. Tang X, Yoshida S, Hsu J, et al. Multi-contrast multi-atlas parcellation of diffusion tensor imaging of the human brain. PLoS One 2014;9:e96985.
31. Fountas KN, Smith JR, Lee GP. Bilateral stereotactic amygdalotomy for self-mutilation disorder. Case report and review of the literature. Stereotact Funct Neurosurg 2007;85:121-8.
32. Wolff JJ, Hazlett HC, Lightbody AA, et al. Repetitive and self-injurious behaviors: associations with caudate volume in autism and fragile X syndrome. J Neurodev Disord 2013;5:12.
33. Duerden EG, Card D, Roberts SW, et al. Self-injurious behaviours are associated with alterations in the somatosensory system in children with autism spectrum disorder. Brain Struct Funct 2014;219:1251-61.
34. Schretlen DJ, Varvaris M, Ho TE, et al. Regional brain volume abnormalities in Lesch-Nyhan disease and its variants: a cross-sectional study. Lancet Neurol 2013;12:1151-8.
35. Faria AV, Zhang J, Oishi K, et al. Atlas-based analysis of neurodevelopment from infancy to adulthood using diffusion tensor imaging and applications for automated abnormality detection. Neuroimage 2010;52:415-28.
36. Deon LL, Kalichman MA, Booth CL, et al. Pallidal deep-brain stimulation associated with complete remission of self-injurious behaviors in a patient with Lesch-Nyhan syndrome: a case report. J Child Neurol 2012;27:117-20.
37. Sotak CH. The role of diffusion tensor imaging in the evaluation of ischemic brain injury - a review. NMR Biomed 2002;15:561-9.
38. Mascalchi M, Filippi M, Floris R, et al. Diffusion-weighted MR of the brain: methodology and clinical application. Radiol Med 2005;109:155-97.
39. Green HA, Pena A, Price CJ, et al. Increased anisotropy in acute stroke: a possible explanation. Stroke 2002;33:1517-21.
40. Boscolo Galazzo I, Brusini L, Obertino S, et al. On the viability of diffusion MRI-based microstructural biomarkers in ischemic stroke. Front Neurosci 2018;12:92.
41. Taylor KI, Sambataro F, Boess F, et al. Progressive decline in gray and white matter integrity in de novo Parkinson's disease: an analysis of longitudinal Parkinson progression markers initiative diffusion tensor imaging data. Front Aging Neurosci 2018;10:318.
42. Liu CB, Yang DG, Zhang X, et al. Degeneration of white matter and gray matter revealed by diffusion tensor imaging and pathological mechanism after spinal cord injury in canine. CNS Neurosci Ther 2019;25:261-72.
43. Fabiano AJ, Horsfield MA, Bakshi R. Interhemispheric asymmetry of brain diffusivity in normal individuals: a diffusion-weighted MR imaging study. Am J Neuroradiol 2005;26:1089-94.